Journal of
Oral Pathology & Medicine

doi: 10.1111/jop.12180

J Oral Pathol Med (2014) 43: 619–626

wileyonlinelibrary.com/journal/jop

Transcriptional profiles of SHH pathway genes in keratocystic odontogenic tumor and ameloblastoma

Clarissa Araújo Silva Gurgel[1], Marcilei Eliza Cavichiolli Buim[2], Kátia Cândido Carvalho[3], Caroline Brandi Schlaepfer Sales[4], Mitermayer Galvão Reis[4], Renata Oliveira de Souza[4], Ludmila de Faro Valverde[4], Roberto Almeida de Azevedo[1], Jean Nunes dos Santos[1], Fernando Augusto Soares[2,5], Eduardo Antônio Gonçalves Ramos[4]

[1]*School of Dentistry of the Federal University of Bahia, Bahia, Brazil;* [2]*AC Camargo Cancer Center, São Paulo, Brazil;* [3]*School of Medicine of the University of São Paulo, São Paulo, Brazil;* [4]*Laboratory of Pathology and Molecular Biology, Oswaldo Cruz Foundation, Bahia, Brazil;* [5]*School of Dentistry of the University of São Paulo, São Paulo, Brazil*

BACKGROUND: Sonic hedgehog (SHH) pathway activation has been identified as a key factor in the development of many types of tumors, including odontogenic tumors. Our study examined the expression of genes in the SHH pathway to characterize their roles in the pathogenesis of keratocystic odontogenic tumors (KOT) and ameloblastomas (AB).

METHODS: We quantified the expression of SHH, SMO, PTCH1, SUFU, GLI1, CCND1, and BCL2 genes by qPCR in a total of 23 KOT, 11 AB, and three non-neoplastic oral mucosa (NNM). We also measured the expression of proteins related to this pathway (CCND1 and BCL2) by immunohistochemistry.

RESULTS: We observed overexpression of SMO, PTCH1, GLI1, and CCND1 genes in both KOT (23/23) and AB (11/11). However, we did not detect expression of the SHH gene in 21/23 KOT and 10/11 AB tumors. Low levels of the SUFU gene were expressed in KOT ($P = 0.0199$) and AB ($P = 0.0127$) relative to the NNM. Recurrent KOT exhibited high levels of SMO ($P = 0.035$), PTCH1 ($P = 0.048$), CCND1 ($P = 0.048$), and BCL2 ($P = 0.045$) transcripts. Using immunolabeling of CCND1, we observed no statistical difference between primary and recurrent KOT ($P = 0.8815$), sporadic and NBCCS-KOT ($P = 0.7688$), and unicystic and solid AB ($P = 0.7521$).

CONCLUSIONS: Overexpression of upstream (PTCH1 and SMO) and downstream (GLI1, CCND1 and BCL2) genes in the SHH pathway leads to the constitutive activation of this pathway in KOT and AB and may suggest a mechanism for the development of these types of tumors.

J Oral Pathol Med (2014) **43:** 619–626

Correspondence: Clarissa Araújo Silva Gurgel, PhD, Laboratory of Oral Surgical Pathology, School of Dentistry of the Federal University of Bahia, Av. Araújo Pinho, 62, Canela, Salvador, Bahia 40110-150, Brazil. Tel: +55 71 3283 9019; +55 75 3224 8350, Fax: +55 71 3283 8964; +55 75 3224 8350, E-mails: clarissagurgelrocha@gmail.com; cgurgel@ufba.br
Accepted for publication February 11, 2014

Keywords: ameloblastoma; keratocystic odontogenic tumor; odontogenic tumors; sonic hedgehog

Introduction

Keratocystic odontogenic tumors (KOT) and ameloblastomas (AB) are a heterogeneous group of tumors that affect jawbones, mainly causing the proliferation of remnants of the dental lamina (1, 2). They show an infiltrative growth, promote local bone destruction, and have high recurrence rates (2). Keratocystic odontogenic tumors is one of the most significant clinical findings in nevoid basal cell carcinoma syndrome (NBCCS) (3, 4), and AB can also represent a clinical finding of this syndrome (5, 6).

Aberrant activation of the SHH signaling pathway during adult life is related to tumor formation (7–9), and disturbances in this pathway have been described as potential factors involved in the pathogenesis of odontogenic tumors (10). The SHH pathway is important for normal development of human tissues (8, 10), such as nerves, the gastrointestinal system, the lungs, and teeth (10). Its primary function is to coordinate the growth of embryonic tissues with that of the mesenchyme (8–10), by the transcriptional activation of genes involved in proliferation (9, 11, 12), apoptosis (12–14), and self-renewal (8–11, 15). Not surprisingly, mutations causing constitutive activation in the SHH pathway are associated with the development of tumor cells in many human malignancies (11, 16). In tissue homeostasis, the PTCH1 protein is an inhibitor of SHH pathway; it represses SMO receptor signaling (7, 17, 18). However, in the presence of SHH ligand, the SHH-PTCH1 complex is internalized, the repression of PTCH1 and SMO is suppressed (8, 10, 17), and molecular signals are transduced to the nucleus by Gli 1, 2, and 3 (7, 17).

Characterizing the transcriptional profiles of genes in the SHH pathway in KOT and AB remains an important knowledge gap in our understanding of the pathogenesis of odontogenic tumors. Our study aimed to characterize the potential role of the genes involved in the SHH pathway, in

attempt to contribute to the knowledge of biologic profile of KOT and AB. Gene expression studies provide important contributions of specific genes involved in the pathogenesis and biologic behavior of KOT and AB. In KOT and AB, several studies have been performed to evaluate loss of heterozygosity, mutations, and polymorphisms of SHH genes, especially PTCH1 (19–24), and examine the expression of proteins involved in this pathway to identify possible mechanisms for the development of these tumor types (25, 26). However, a close examination of the expression profile of SHH genes by a sensitive method such as qPCR has never been evaluated in KOT and AB. As SHH pathways genes represent druggable targets (27), it is important to identify molecules in this signaling cascade that provide an opportunity for pharmacological intervention prior to surgery.

Materials and methods

Sample collection

This study was approved by the Ethics Committee of the Gonçalo Moniz Research Center, Oswaldo Cruz Foundation. A total of 23 KOT and 11 AB were collected between 2007 and 2010 along with relevant clinical data. The KOT were classified as sporadic (n = 18) or NBCCS-KOT (n = 5) using previously described criteria for this syndrome (28). In the sporadic group, KOT were classified as primary (n = 10), if they had not received treatment previously or, recurrent (n = 8), if patients had received prior treatment. KOT recurrences occurred at 24 month on average following the initial treatment. All AB were primary and classified by an experienced pathologist as solid type (n = 6) or unicystic (n = 5). KOT and unicystic AB were previously treated by enucleation, and solid AB were removed by surgical resection with a safety margin of at least 1 cm. Main Clinical data are summarized in Table 1. Three NNM oral mucosa were donated by healthy individuals undergoing extraction of third molars for orthodontic reasons. All samples were previously diagnosed as KOT or AB by incisional biopsy and were immediately snap-frozen in liquid nitrogen following surgery and stored at −80°C until RNA could be extracted.

Table 1 Main clinical data

	Keratocystic odontogenic tumor	*Ameloblastoma*
Clinical data	*n%*	*n%*
Gender		
Male	10 (43.5)	4 (36.4)
Female	13 (56.5)	7 (63.6)
Age (years)		
<18	5 (21.74)	0 (0.0)
19–35	9 (39.12)	6 (54.5)
36–50	6 (26.1)	4 (36.4)
>50	3 (13.04)	1 (9.1)
Location		
Mandible posterior	19 (82.60)	10 (90.9)
Mandible anterior	1 (4.35)	1 (9.1)
Maxilla posterior	3 (13.05)	0 (0.0)
Maxilla anterior	0 (0.0)	0 (0.0)
Treatment modality		
Enucleation with curettage	23 (100.0)	5 (45.5)
Resection	0 (0)	6 (54.5)
Follow-up (months)		
<12	10 (43.5)	5 (45.45)
12–24	8 (34.8)	5 (45.5)
>24	4 (17.4)	1 (9.1)
No information	1 (4.3)	0 (0.0)

RNA extraction and reverse transcription

Total RNA was extracted from 25 to 30 mg of frozen KOT and AB according to the manufacturer's specifications (RNeasy Mini Kit, Qiagen, Hilden, DE). The samples were first pulverized with mortar and pestle that had been treated with 0.1% DEPC prior to sample processing. Genomic DNA was eliminated by the enzyme DNase I (1 μg: 1 μL proportion of the template and enzyme) (DNase I Amplification Grade kit, Invitrogen, Carlsbad, CA). The amount and purity of the RNA was assessed using spectrophotometry (NanoDrop, Thermo Scientific, Wilmington, DE, USA), and purity was considered satisfactory when the A260/A280 ratio = 1.9–2.05. Integrity of total RNA was confirmed on an agarose gel (containing 1% formaldehyde). Total RNA was stored in 30 μl of RNase-free water (RNeasy Mini Kit, Qiagen, Hilden, DE) at −80°C. First-strand cDNA was synthesized from 2 μg of total RNA using oligo (dT) primers and the Superscript II Reverse Transcriptase Kit (Invitrogen) in a reaction volume of 20 μl according to the protocol provided by the manufacturer. Reaction mixtures were incubated at 42°C for 2 min, followed by 65°C for 50 min, 42°C for 55 min, 70°C for 15 min, 37°C for 20 min, and 4°C for 5 min. The cDNA was stored at −20°C. Reverse transcriptase efficiency was assessed by the amplification of the GAPDH and ACTB reference genes.

Quantitative real-time polymerase chain reaction (qPCR)

Primers for SHH, SMO, SUFU, PTCH1, GLI1, CCND1, BCL2 and the GAPDH, ACTB, and HPRT1 controls were designed using the Primer Express software 3.0 (Applied Biosystems, Foster City, CA, USA) based on sequences in GenBank *(*http://www.ncbi.nlm.nih.gov/genbank/) and validated *in silico* using BLAT (http://genome.ucsc.edu/cgibin/hgBlat?command=start). All qPCR primers were synthesized at Integrated DNA Technologies (IDT, San Diego, CA, USA) and are listed in Table 2.

Three endogenous genes (ACTB, GAPDH, and HPRT1) were tested as normalizers in all samples. The amplification curves were analyzed using GeNorm™ software (29), and the GAPDH gene yielded the most reproducible results. A relative standard curve was constructed for testing the efficiency of all primers, using a serial dilution of a small cell lung cancer line (H146) (100, 50, 25, 12.5, and 6.25 ng/μl). The standard curves of the targets and references genes yielded similar efficiencies ($-3.6 \geq$ slope ≥ -3.3).

Quantitative PCR assays were conducted in duplicate in an ABI Prism 7900 Sequence Detection System (Applied Biosystems). PCRs were performed in a total volume of 20 μl, containing 10 ng of cDNA sample (total RNA equivalents), 0.2 μM of each of the primers, and 1X of the SYBR-Green PCR Master Mix Kit (Applied Biosystems). The amplification program consisted of one cycle of 50°C for 2 min and 95°C for 10 min, followed by 40 cycles of 95°C for 15 s and 60°C for 1 min. To verify the

Table 2 Primer sequences used for mRNA expression analysis with gene name

Identification	*Accession Number*	*Sequences 5′→3′*
Sonic hedgehog homolog (Drosophila) (SHH)	NM_000193.2	F: GCGCCAGCGGAAGGTAT R: CCGGTGTTTTCTTCATCCTTAAA
Patched homolog 1 (PTCH1)	NM_000264.3	F: GGGTGGCACAGTCAAGAACAG R: CGTACATTTGCTTGGGAGTCATT
Smoothened homolog (Drosophila) (SMO)	NM_005631.3	F: GGTTTGTGGTCCTCACCTATGC R: GGAGGTCTTGCCCGAGAGA
Suppressor of fused homolog (Drosophila) (SUFU)	NM_016169.2	F: GAGGACAGCCGGAGCATCT R: AGGACAGGTTTGCTGTTGATCTC
Glioma-associated oncogene homolog 1 (GLI1)	NM_005269.1	F: CGCTGCGAAAACATGTCAAG R: CCACGGTGCCGTTTGGT
Cyclin D1 (CCND1)	NM_053056.2	F: CAAACAGATCATCCGCAAACA R: ACTCCAGCAGGGCTTCGAT
B-cell CLL/lymphoma 2 (BCL2)	NM_000633.2	F: CCTGTGGATGACTGAGTACCTGAA R: GGGCCGTACAGTTCCACAAA
Glyceraldehyde-3-phosphate dehydrogenase (GAPDH)	NM_002046	F: CCAGGTGGTCTCCTCTGACTTC R: GTGGTCGTTGAGGGCAATG
Hypoxanthine phosphoribosyltransferase 1 (HPRT1)	NM_000194	F: GCTCGAGATGTGATGAAGGAGAT R: CCAGCAGGTCAGCAAAGAATT
β-actin (ACTB)	NM_001101.3	F: GCACCCAGCACAATGAAG R: CTTGCTGATCCACATCTGC

F, forward; R, reverse.

amplification specificity, we performed melting curve analyses using initial denaturation at 95°C for 15 s followed by 15 s at 60°C and then heated the samples at 95°C at a slow rate of 0.1°C/s with continuous fluorescence detection. The positive control consisted of a pool of two KOT and one AB that were positive for all mRNA targets.

Relative quantification was given by the ratio between the mean value of the target gene and the value of the reference gene (GAPDH) in each sample. All reactions were baseline corrected, and the identical threshold was set manually for each gene in all samples. The relative gene expression was also normalized on the basis of the expression of a reference sample/calibrator (pool of NNM). The relative amount of PCR product generated from each primer set was determined on the basis of the Cq values, and relative quantification was calculated by a mathematical model, previously described by Pfaffl (30).

Immunohistochemistry

Immunostaining was performed for CCND1 and BCL2 using the streptavidin–biotin complex (LSAB, DakoCytomation, Glostrup, DK). Sections were treated to remove paraffin, rehydrated, and washed in distilled water. Antigen retrieval was performed with a sodium citrate solution (pH 6.0) heated to 96°C for 30 min. Slides were then incubated with primary antibodies (Table 3) for 60 min in a humid chamber, at room temperature (RT). Then, the slides were washed with 1% PBS/BSA and incubated with a pool of biotinylated secondary antibodies (Link reagent, DakoCytomation, Glostrup, Denmark) for 60 min, at RT, followed by washing and incubation with the streptavidin–biotin–peroxidase complex. Staining was revealed by incubating the slides in 3, 3′ diaminobenzidine solution (Dako, Carpinteria, CA, USA). The slides were counterstained with hematoxylin, dehydrated in absolute ethanol and xylene, mounted with cover slips using a permanent mounting medium, and observed using an optical light microscope. As positive control, a fragment squamous cell carcinoma was used for both CCND1 and BCL2. The negative control consisted of replacement of the primary antibody with an isotype-matched control antibody.

Table 3 Antibodies used in the study and their respective clones, dilutions, and manufacturer

Antibody	*Clone*	*Dilution*	*Source*
CCND1	DCS6	1:100	DakoCytomation, Glostrup, Denmark
BCL2	124	1:50	DakoCytomation, Glostrup, Denmark

Using the capture system Axio-Zeiss 4.04 (ZEISS, Jena, Germany, 2004), immunostaining analysis was performed by one observer in 10 microscopic fields at a final magnification of 400×. A minimum of 500 epithelial nuclei from KOT and AB were analyzed in representative areas of tumors by the software Image Tool 2.0 (UTHSCSA, Texas University, TX, USA, 1996). Positive cells located on basal and suprabasal layers were counted for KOT cases, and those located on stellate reticulum and more peripheral layers were scored for AB cases. Semiquantification was obtained by attributing four scores: (−) no expression; +1, <20% positive cells; +2, 21–50% positive cells, and +3, >50% positive cells (31).

Statistical analysis

As the mRNA and protein expression was not normally distributed (Kolmogorov–Smirnov test, $P < 0.001$), the association between genes expression and clinical pathological parameters was assessed using the Mann–Whitney and Kruskal–Wallis test. The correlation between expression of different genes was determined using the Spearman test. All P values were based on two-tailed statistical

analyses, and $P < 0.05$ was considered to be statistically significant. The statistical calculation was performed using the GraphPad Prism 5.01 (San Diego, CA, USA).

Result

SHH pathway gene expression profiles indicate activation of this pathway in KOT and AB

To characterize the expression profiles of genes in the SHH pathway in two tumor types, we performed qPCR on total RNA isolated from 23 KOT and 11 AB. As shown in Fig. 1, we observed overexpression of SMO, PTCH1, GLI1, and CCND1 genes in all KOT ($n = 23$) and AB ($n = 11$). We detected low levels of SUFU mRNA in all KOT and AB when we compared expression in tumors to non-neoplastic tissue ($P = 0.019$ and $P = 0.012$, respectively). We also found that the BCL2 gene was highly expressed in KOT ($n = 23$) and AB ($n = 11$), but there was no statistical difference between tumors and NNM. Despite our observation that multiple genes in the SHH pathway are activated in tumors, we detected no SHH gene expression (high Cq values; qPCR cycle >32) in 21 (91.3%) KOT and 10 (90.9%) AB, and only low expression of the SHH gene in two NBCCS-KOT and one AB. Median relative expression level of all studied genes was similar for solid and unicystic AB as well as KOT and AB. We did not observe expression of the SHH, SMO, PTCH1, or GLI1 genes in NNM (qPCR cycle >32 for all these transcripts) (Fig. 1).

Recurrent KOT exhibited high levels of SMO, PTCH1, CCND1, and BCL2 genes

Recurrent KOT ($n = 8$) exhibited high levels of SMO ($P = 0.035$), PTCH1 ($P = 0.048$), CCND1 ($P = 0.048$), and BCL2 ($P = 0.045$) transcripts (Fig. 2). We found no statistical differences in the expression of GLI1 and SUFU genes between recurrent and primary KOT nor did we find any differences in mRNA expression for any of the aforementioned genes in NBCCS-KOT and sporadic KOT (Fig. 2). We observed a positive correlation between the expression of SMO and GLI1 genes (rs = 0.687, $P = 0.00$) in KOT. We found no correlation in gene expression in the AB group or other genes in KOT.

Suprabasal cells and cells similar to pre-ameloblasts represent the proliferative components in KOT and AB

In KOT, we determined that the CCND1 protein was localized in the nucleus and cytoplasm, especially in suprabasal layers (Fig. 3). A majority of the labeled protein (score +3) localized to the nucleus (83%; $n = 19$) in all NBCCS-KOT. We also measured CCND1 in the cytoplasm (score +2) in over half of the KOT (65%; $n = 15$). We found no statistical difference in the immunostaining of CCND1 between primary and recurrent KOT (Mann–Whitney test, $P = 0.88$), or between sporadic and NBCCS-KOT (Mann–Whitney test, $P = 0.7688$). In AB, we observed nuclear (score +2) and cytoplasmic localization (score +3) of CCND1 in nearly half of the cells which shared similar characteristics to pre-ameloblasts (45%, $n = 5$) (Fig. 3). No statistical difference between unicystic and solid AB subtypes was found (Mann–Whitney test, $P = 0.75$).

The BCL2 protein was localized exclusively in the basal layer on cystic epithelial lining of 52.17% ($n = 12$) KOT and assigned a score +1. We observed cytoplasmic and nuclear immunostaining for BCL2 (score +3 and +2, respectively) in 90.9% ($n = 10$) of AB cases, especially in cells similar to pre-ameloblasts ($n = 8$; 72.72%) (Fig. 3).

Discussion

Many signaling pathways that participate actively in the formation of human embryonic tissues are kept 'off' in adult cells as aberrant activation of these pathways can result in tumor development (8–10) and maintenance of a tumor cell phenotype (7, 8, 15). In AB (32) and KOT, mutations in PTCH1 gene have been reported, especially in patients with NBCCS (19, 20, 22, 23, 33). These data prompted our investigation of the role of the SHH pathway in tumors associated with this syndrome, such as AB (5, 6). In this study, we showed that several of the genes involved in the SHH pathway are differentially expressed in KOT and AB. We demonstrated overexpression of SMO, PTCH1, GLI1, CCND1 genes and a loss of expression of SUFU gene in KOT and AB indicating that these SHH pathway genes contribute to the development and biologic

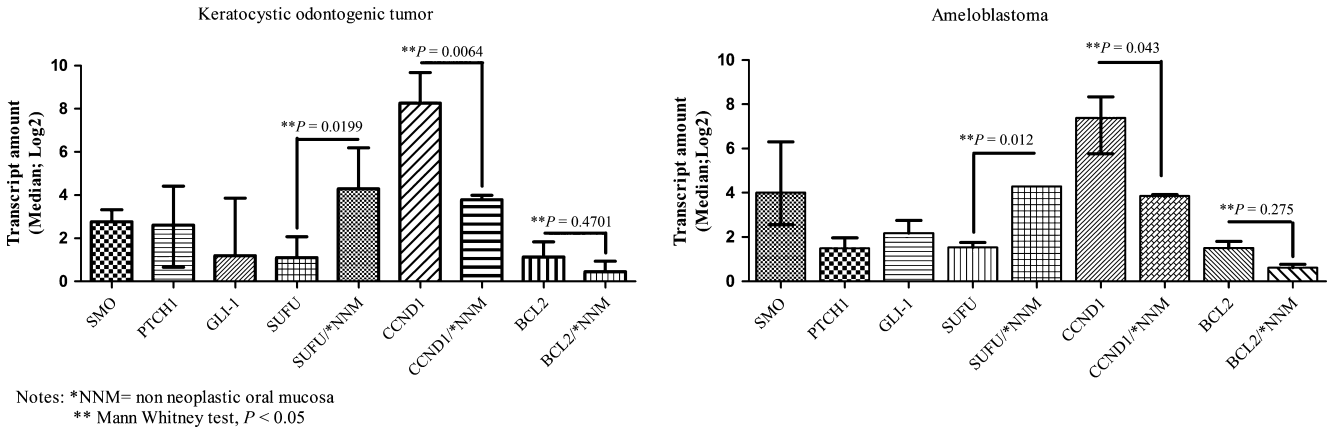

Notes: *NNM= non neoplastic oral mucosa
** Mann Whitney test, $P < 0.05$

Figure 1 Expression profile of SHH pathway genes and comparison of transcript amount of SUFU, CCND1, and BCL2 genes in keratocystic odontogenic tumors (KOT) and ameloblastomas (AB) in relation to non-neoplastic oral mucosa (NNM).

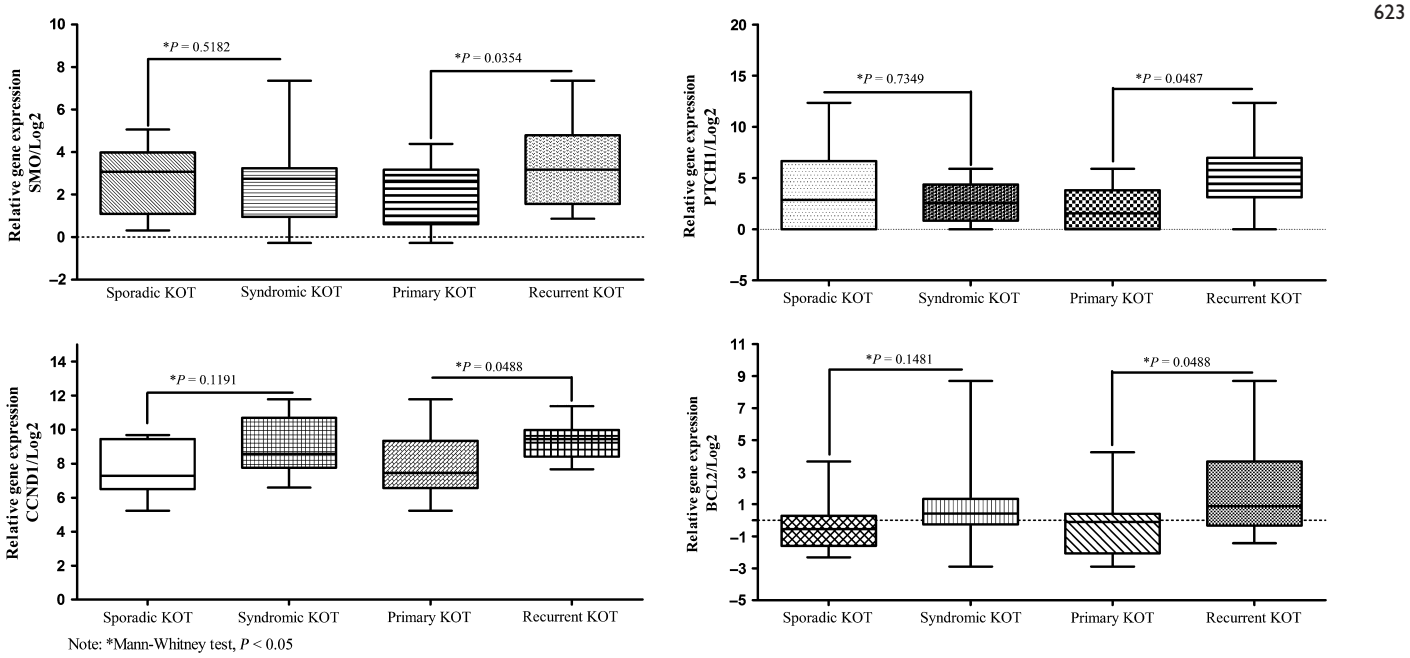

Figure 2 Comparative expression of SMO, PTCH1, CCND1, and BCL2 genes in primary, recurrent, sporadic, and syndromic keratocystic odontogenic tumors (KOT).

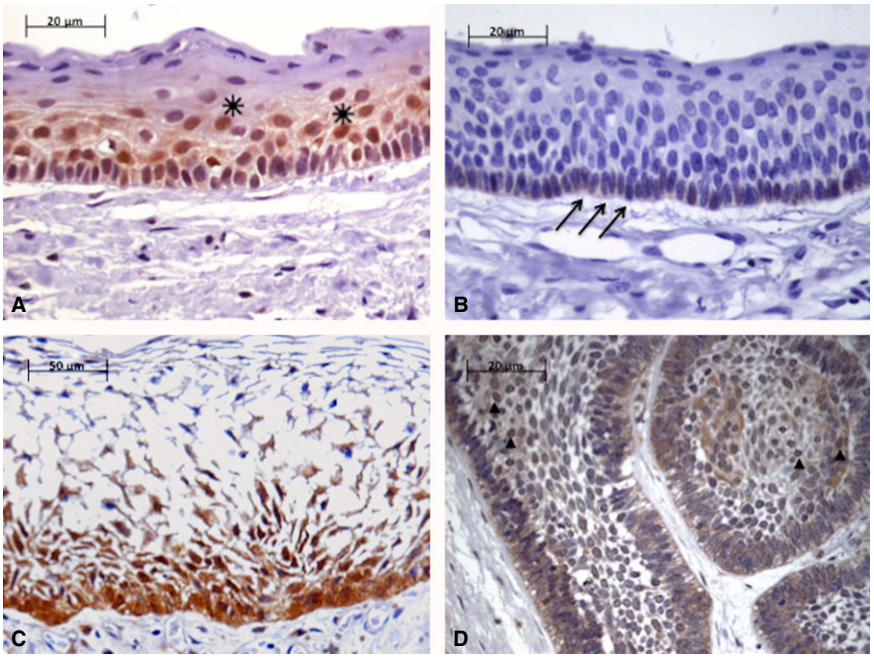

Figure 3 KOT- (A) CCND1 protein in the nucleus and cytoplasm, especially in suprabasal layers (asterisks). (B) BCL2 protein is present only in the basal layer on cystic epithelial cells (arrows). AB- (C) CCND1 protein in nucleus and cytoplasm of unicystic AB. (D) Cytoplasmic and nuclear staining for BCL2 protein in solid AB (arrowhead).

behavior of these tumors. Our results provide important insights into the role of these genes in tumorigenesis of odontogenic tumors.

Up-regulation of the SMO gene is one mechanism for altering SHH pathway activity (34, 35). In basal cell carcinoma (34) and pancreatic cancer (36), tumor pathogenesis and proliferation occurs as a result of gain of function mutations that result in up-regulation of the SMO gene, but the role of this gene in KOT and AB is not well characterized (23). Meanwhile, overexpression of PTCH1 gene in KOT and AB should be better investigated to evaluate if mutation in other genes involved in SHH pathway could induce PTCH1 up-regulation. Our results also confirm previous findings that PTCH1 (10, 37), CCND1 (9, 11), and BCL2 (9, 12) genes are also target genes in the SHH signaling cascade (11, 34, 37, 38) and suggest a possible role of this cascade in proliferation and cell survival in KOT and AB.

Additionally, the contribution of SUFU gene to KOT and AB pathogenesis remains unclear (39). Loss of SUFU expression has been reported in other tumor types (39, 40) and the phenotype of these tumors is similar to those resulting from decreased PTCH1 expression in humans and NBCCS in rodents (41). Thus, this gene requires further investigation in these tumors to define its role in tumorigenesis.

GLI1 transcription factor activity mediates pathological responses to deregulate SHH signaling in humans, and this molecule therefore represents a putative therapeutic target for odontogenic tumors. The expression of GLI1 molecule serves as a marker for the activity of the SHH pathway and is correlated with activation of genes involved in cell proliferation and survival (11, 12). CCND1 and BCL2 are target genes of GLI1 transcription factor (9, 11, 12), and one consequence of deregulated SHH pathway is the up-regulation of genes in this pathway as we showed in these studies. Up-regulation of the CCND1 gene reduces the dependence of mitogens for signaling pathway activation and is the key player in cell cycle progression to S phase (42). The BCL2 protein is related with cell survival and cell differentiation and expression of the BCL2 gene might be regulated by transcriptional activation of GLI1 (43). However, the expression of the CCND1 and BCL2 target genes may be controlled by more one transcription factor such as NK-kB and STAT3 (44, 45).

We showed a higher expression of CCND1 protein in cells similar to pre-ameloblasts indicating that these cells are primarily responsible for tumor growth in AB. *Supra*basal cells seem to play this role in KOT as demonstrated in other studies involving cell proliferation markers (2, 31, 42, 46). In KOT, there was no statistical difference when the primary and recurrent groups, sporadic and syndromic KOT were compared. This is different to results from Kimi et al. (42) that showed increased CCND1 protein expression in NBCCS-KOT.

We also observed positive CCND1 protein in the cytoplasm of KOT and AB cells. To date, evidence suggests that nuclear retention is critical for oncogenic function by CCND1 (42, 47). For example, when a mutant CCND1 protein, resistant to proteolytic degradation, was expressed, the localization of the protein was altered from nuclear to nuclear and cytoplasmic (47) Therefore, our observation that there is overexpression of CCND1 protein suggests that the progression of neoplastic cells, in KOT and AB, starts at a step preceding the checkpoint coordinated by p53 protein.

In KOT, BCL2 immunostaining was only observed in basal cells corroborating with others studies (42, 48, 49) and indicating that the cell differentiation mechanisms may be present in progenitor cells. Similar to Luo et al. (50), predominance of BCL2 in pre-ameloblasts-like cells in our AB samples indicates that cell survival is also prevalent in this cell type, regardless either unicystic or solid ameloblastoma. The nuclear localization observed may be related to the function of BCL2 in the DNA protection when under the action of endonucleases and is more common in malignant processes (51) and need to be better evaluated in AB.

Our results showed an overexpression of SMO, PTCH1, CCND1, and BCL2 genes in recurrent KOT. Recurrence is a well-described event in KOT and related with surgery type (52–56) as well as biologic profile of tumor (57–60). Previously, SMO protein localization studies showed that recurrence of KOT is associated with strong SMO detection and higher Ki-67 labeling (26). Aggressive behavior and high recurrence rates of this tumor are thought to be due to marked proliferative activity of tumor cells (25, 58). Although previous studies are unable to find a difference in Ki-67 and p53 in primary and recurrent KOT (31), others have concluded that higher SMO expression could be a possible factor associated with frequent recurrence of KOT (23). Thus, neoplastic cells with aberrant SHH pathway can proliferate quickly re-establishing the tumor in a short time.

The high Cq values observed for the SHH gene in KOT and AB indicate a very small amount of SHH mRNA in both tumors. As the reference gene GAPDH was successful amplified in all samples, the amount of RNA did not appear to be a limiting factor. In embryonic tissues, SHH pathway can be activated by SHH ligand and the expression of this in mRNA level is not detected in normal adult tissues (7, 8, 10, 17). However, previous studies in KOT and AB yielded conflicting results. According to Grachtchouk et al. (38), SHH transcript was not detected in mouse KOT epithelium or surrounding stroma. Ohki et al. (21) and Kumamoto et al. (61) detected mRNA transcript of SHH in KOT and AB, respectively. Other studies demonstrated a very low expression of SHH gene in AB (62, 63).

It is possible that different techniques used to investigate SHH gene expression could explain the differences in the reported results. The hypermethylation of the SHH gene (64) results in undetected expression of the SHH gene (65) and warrants further evaluation in KOT and AB. In addition, future studies might utilize digital PCR to better analyze levels of the SHH gene transcript in both tumors and also probe microRNA regulation.

Finally, our results suggest the potential role of overexpression of upstream (PTCH1 and SMO) and downstream (GLI1, CCND1, and BCL2) genes in KOT and AB, leading to the constitutive activation of SHH pathway and contributing to cells proliferation and survival. The research for molecular markers has important clinical implications in the management of KOT and AB. Medicines for blocking this pathway in KOT and AB is a point of interest for an alternative treatment prior to surgery, and SHH genes offer a great opportunity for these tests.

References

1. Mello LA, Gurgel CAS, Ramos EAG, et al. Keratocystic odontogenic tumour: an experience in the Northeast of Brazil. *Srp Arh Celok Lek* 2011; **139**: 291–7.
2. Pan S, Li T-J. PTCH1 mutations in odontogenic keratocysts: are they related to epithelial cell proliferation? *Oral Oncol* 2009; **45**: 861–5.
3. Shimada Y, Morita K, Kabasawa Y, Taguchi T, Omura K. Clinical manifestations and treatment for keratocystic odontogenic tumors associated with nevoid basal cell carcinoma syndrome: a study in 25 Japanese patients. *J Oral Pathol Med* 2013; **42**: 275–80.
4. Suzuki M, Nagao K, Hatsuse H, et al. Molecular pathogenesis of keratocystic odontogenic tumors developing in nevoid basal cell carcinoma syndrome. *Oral Surg Oral Med Oral Pathol Oral Radiol* 2013; **116**: 348–53.

5. Eslami B, Lorente C, Kieff D, Caruso PA, Faquin WC. Ameloblastoma associated with the nevoid basal cell carcinoma (Gorlin) syndrome. *Oral Surg Oral Med Oral Pathol Oral Radiol Endod* 2008; **105**: e10–13.
6. Ponti G, Pastorino L, Pollio A, et al. Ameloblastoma: a neglected criterion for nevoid basal cell carcinoma (Gorlin) syndrome. *Fam Cancer* 2012; **11**: 411–18.
7. Ingham PW, McMahon AP. Hedgehog signaling in animal development: paradigms and principles. *Genes Dev* 2001; **15**: 3059–87.
8. Chari NS, McDonnell TJ. The sonic hedgehog signaling network in development and neoplasia. *Adv Anat Pathol* 2007; **14**: 344–52.
9. Katoh Y, Katoh M. Hedgehog target genes: mechanisms of carcinogenesis induced by aberrant hedgehog signaling activation. *Curr Mol Med* 2009; **9**: 873–86.
10. Cohen MM. Hedgehog signaling update. *Am J Med Genet A* 2010; **152A**: 1875–914.
11. Kasper M, Regl G, Frischauf A-M, Aberger F. GLI transcription factors: mediators of oncogenic Hedgehog signalling. *Eur J Cancer* 2006; **42**: 437–45.
12. Stecca B, Ruiz I, Altaba A. Context-dependent regulation of the GLI code in cancer by HEDGEHOG and non-HEDGEHOG signals. *J Mol Cell Biol* 2010; **2**: 84–95.
13. Ruizi Altaba A. The works of GLI and the power of hedgehog. *Nat Cell Biol* 1999; **1**: E147–8.
14. Ruizi Altaba A, Sánchez P, Dahmane N. Gli and hedgehog in cancer: tumours, embryos and stem cells. *Nat Rev Cancer* 2002; **2**: 361–72.
15. Adolphe C, Narang M, Ellis T, Wicking C, Kaur P, Wainwright B. An *in vivo* comparative study of sonic, desert and Indian hedgehog reveals that hedgehog pathway activity regulates epidermal stem cell homeostasis. *Development* 2004; **131**: 5009–19.
16. Thayer SP, di Magliano MP, Heiser PW, et al. Hedgehog is an early and late mediator of pancreatic cancer tumorigenesis. *Nature* 2003; **425**: 851–6.
17. Wetmore C. Sonic hedgehog in normal and neoplastic proliferation: insight gained from human tumors and animal models. *Curr Opin Genet Dev* 2003; **13**: 34–42.
18. Taipale J, Cooper MK, Maiti T, Beachy PA. Patched acts catalytically to suppress the activity of Smoothened. *Nature* 2002; **418**: 892–7.
19. Lench NJ, High AS, Markham AF, Hume WJ, Robinson PA. Investigation of chromosome 9q22.3-q31 DNA marker loss in odontogenic keratocysts. *Eur J Cancer B Oral Oncol* 1996; **32B**: 202–6.
20. Barreto DC, Bale AE, De Marco L, Gomez RS. Immunolocalization of PTCH protein in odontogenic cysts and tumors. *J Dent Res* 2002; **81**: 757–60.
21. Ohki K, Kumamoto H, Ichinohasama R, Sato T, Takahashi N, Ooya K. PTC gene mutations and expression of SHH, PTC, SMO, and GLI-1 in odontogenic keratocysts. *Int J Oral Maxillofac Surg* 2004; **33**: 584–92.
22. Gu X-M, Zhao H-S, Sun L-S, Li T-J. PTCH mutations in sporadic and Gorlin-syndrome-related odontogenic keratocysts. *J Dent Res* 2006; **85**: 859–63.
23. Sun L-S, Li X-F, Li T-J. PTCH1 and SMO gene alterations in keratocystic odontogenic tumors. *J Dent Res* 2008; **87**: 575–9.
24. Farias LC, Gomes CC, Brito JAR, et al. Loss of heterozygosity of the PTCH gene in ameloblastoma. *Hum Pathol* 2012; **43**: 1229–33.
25. Yagyuu T, Kirita T, Sasahira T, Moriwaka Y, Yamamoto K, Kuniyasu H. Recurrence of keratocystic odontogenic tumor: clinicopathological features and immunohistochemical study of the Hedgehog signaling pathway. *Pathobiology* 2008; **75**: 171–6.
26. Vered M, Peleg O, Taicher S, Buchner A. The immunoprofile of odontogenic keratocyst (keratocystic odontogenic tumor) that includes expression of PTCH, SMO, GLI-1 and bcl-2 is similar to ameloblastoma but different from odontogenic cysts. *J Oral Pathol Med* 2009; **38**: 597–604.
27. Scales SJ, de Sauvage FJ. Mechanisms of Hedgehog pathway activation in cancer and implications for therapy. *Trends Pharmacol Sci* 2009; **30**: 303–12.
28. High A, Zedan W. Basal cell nevus syndrome. *Curr Opin Oncol* 2005; **17**: 160–6.
29. Vandesompele J, De Preter K, Pattyn F, et al. Accurate normalization of real-time quantitative RT-PCR data by geometric averaging of multiple internal control genes. *Genome Biol* 2002; **3**: RESEARCH0034.
30. Pfaffl MW. *A new mathematical model for relative quantification in real-time RT–PCR*. Moore JD, Stenning K, editors. *Nucleic Acids Res*. Oxford University Press; 2001;**29**:e45.
31. Gurgel CAS, Ramos EAG, Azevedo RA, Sarmento VA, da Silva Carvalho AM, dos Santos JN. Expression of Ki-67, p53 and p63 proteins in keratocyst odontogenic tumours: an immunohistochemical study. *J Mol Histol* 2008; **39**: 311–16.
32. Ponti G, Pollio A, Mignogna MD, et al. Unicystic ameloblastoma associated with the novel K729M PTCH1 mutation in a patient with nevoid basal cell carcinoma (Gorlin) syndrome. *Cancer Genet* 2012; **205**: 177–81.
33. Guo Y-Y, Zhang J-Y, Li X-F, Luo H-Y, Chen F, Li T-J. PTCH1 gene mutations in keratocystic odontogenic tumors: a study of 43 chinese patients and a systematic review. *PLoS ONE* 2013; **8**: e77305.
34. Xie J, Murone M, Luoh SM, et al. Activating Smoothened mutations in sporadic basal-cell carcinoma. *Nature* 1998; **391**: 90–2.
35. Lam CW, Xie J, To KF, et al. A frequent activated smoothened mutation in sporadic basal cell carcinomas. *Oncogene* 1999; **18**: 833–6.
36. Walter K, Omura N, Hong S-M, et al. Overexpression of smoothened activates the sonic hedgehog signaling pathway in pancreatic cancer-associated fibroblasts. *Clin Cancer Res* 2010; **16**: 1781–9.
37. Karhadkar SS, Bova GS, Abdallah N, et al. Hedgehog signalling in prostate regeneration, neoplasia and metastasis. *Nature* 2004; **431**: 707–12.
38. Grachtchouk M, Liu J, Wang A, et al. Odontogenic keratocysts arise from quiescent epithelial rests and are associated with deregulated hedgehog signaling in mice and humans. *Am J Pathol* 2006; **169**: 806–14.
39. Svärd J, Heby-Henricson K, Henricson KH, et al. Genetic elimination of Suppressor of fused reveals an essential repressor function in the mammalian Hedgehog signaling pathway. *Dev Cell* 2006; **10**: 187–97.
40. Taylor MD, Liu L, Raffel C, et al. Mutations in SUFU predispose to medulloblastoma. *Nat Genet* 2002; **31**: 306–10.
41. Varjosalo M, Li S-P, Taipale J. Divergence of hedgehog signal transduction mechanism between Drosophila and mammals. *Dev Cell* 2006; **10**: 177–86.
42. Kimi K, Kumamoto H, Ooya K, Motegi K. Immunohistochemical analysis of cell-cycle- and apoptosis-related factors in lining epithelium of odontogenic keratocysts. *J Oral Pathol Med* 2001; **30**: 434–42.
43. Bigelow RLH, Chari NS, Unden AB, et al. Transcriptional regulation of bcl-2 mediated by the sonic hedgehog signaling pathway through gli-1. *J Biol Chem* 2004; **279**: 1197–205.
44. Yu H, Kortylewski M, Pardoll D. Crosstalk between cancer and immune cells: role of STAT3 in the tumour microenvironment. *Nat Rev Immunol* 2007; **7**: 41–51.
45. Bollrath J, Phesse TJ, von Burstin VA, et al. gp130-mediated Stat3 activation in enterocytes regulates cell survival and

cell-cycle progression during colitis-associated tumorigenesis. *Cancer Cell* 2009; **15**: 91–102.
46. Kumamoto H, Kimi K, Ooya K. Detection of cell cycle-related factors in ameloblastomas. *J Oral Pathol Med* 2001; **30**: 309–15.
47. Fu M, Wang C, Li Z, Sakamaki T, Pestell RG. Minireview: Cyclin D1: normal and abnormal functions. *Endocrinology* 2004; **145**: 5439–47.
48. Kichi E, Enokiya Y, Muramatsu T, et al. Cell proliferation, apoptosis and apoptosis-related factors in odontogenic keratocysts and in dentigerous cysts. *J Oral Pathol Med* 2005; **34**: 280–6.
49. Rangiani A, Motahhary P. Evaluation of bax and bcl-2 expression in odontogenic keratocysts and orthokeratinized odontogenic cysts: a comparison of two cysts. *Oral Oncol* 2009; **45**: e41–4.
50. Luo H-Y, Yu S-F, Li T-J. Differential expression of apoptosis-related proteins in various cellular components of ameloblastomas. *Int J Oral Maxillofac Surg* 2006; **35**: 750–5.
51. Drachenberg CB, Ioffe OB, Castellani RJ, Papadimitriou JC. Nuclear bcl-2 staining in tumors. *Am J Clin Pathol* 1997; **108**: 479.
52. Stoelinga PJ, Bronkhorst FB. The incidence, multiple presentation and recurrence of aggressive cysts of the jaws. *J Craniomaxillofac Surg* 1988; **16**: 184–95.
53. Gupta A, Suvarna S, Khanna G, Sahoo S. Recurrence of keratocyst in nevoid basal cell carcinoma syndrome: a major diagnostic dilemma for clinicians. *J Cancer Res Ther* 2013; **9**: 543–4.
54. Bhargava D, Deshpande A, Pogrel MA. Keratocystic odontogenic tumour (KCOT)-a cyst to a tumour. *Oral Maxillofac Surg* 2012; **16**: 163–70.
55. Pogrel MA. The keratocystic odontogenic tumor. *Oral Maxillofac Surg Clin North Am* 2013; **25**: 21–30, v.
56. Stoelinga PJW. Kaczmarzyc, et al.: A systematic review of the recurrence rate for keratocystic odontogenic tumour in relation to treatment modalities. *Int J Oral Maxillofac Surg* 2012; **41**: 1585–6; author reply 1586–7.
57. Shear M. The aggressive nature of the odontogenic keratocyst: is it a benign cystic neoplasm? Part 1. Clinical and early experimental evidence of aggressive behaviour. *Oral Oncol* 2002; **38**: 219–26.
58. Shear M. The aggressive nature of the odontogenic keratocyst: is it a benign cystic neoplasm? Part 2. Proliferation and genetic studies. *Oral Oncol* 2002; **38**: 323–31.
59. Shear M. The aggressive nature of the odontogenic keratocyst: is it a benign cystic neoplasm? Part 3. Immunocytochemistry of cytokeratin and other epithelial cell markers. *Oral Oncol* 2002; **38**: 407–15.
60. Mendes RA, Carvalho JF, van der Waal I. Biological pathways involved in the aggressive behavior of the keratocystic odontogenic tumor and possible implications for molecular oriented treatment - an overview. *Oral Oncol* 2010; **46**: 19–24.
61. Kumamoto H, Ohki K, Ooya K. Expression of Sonic hedgehog (SHH) signaling molecules in ameloblastomas. *J Oral Pathol Med* 2004; **33**: 185–90.
62. Heikinheimo K, Jee KJ, Niini T, et al. Gene expression profiling of ameloblastoma and human tooth germ by means of a cDNA microarray. *J Dent Res* 2002; **81**: 525–30.
63. DeVilliers P, Suggs C, Simmons D, Murrah V, Wright JT. Microgenomics of ameloblastoma. *J Dent Res* 2011; **90**: 463–9.
64. Brinkhuizen T, van den Hurk K, Winnepenninckx VJL, et al. Epigenetic changes in Basal Cell Carcinoma affect SHH and WNT signaling components. *PLoS ONE* 2012; **7**: e51710.
65. Ten Haaf A, Franken L, Heymann C, et al. Paradox of sonic hedgehog (SHH) transcriptional regulation: alternative transcription initiation overrides the effect of downstream promoter DNA methylation. *Epigenetics* 2011; **6**: 465–77.

Acknowledgements

This study was supported by Fapesb Grants 37808, Bahia, Brazil. We would like to express our sincere thanks to Janet Lindow (Yale School of Public Health) for reviewing this article.